Conformational Analysis

DOI: 10.1002/anie.201408220

A Sharp Thermal Transition of Fast Aromatic-Ring Dynamics in Ubiquitin**

*Vignesh Kasinath, Yinan Fu, Kim A. Sharp, and A. Joshua Wand**

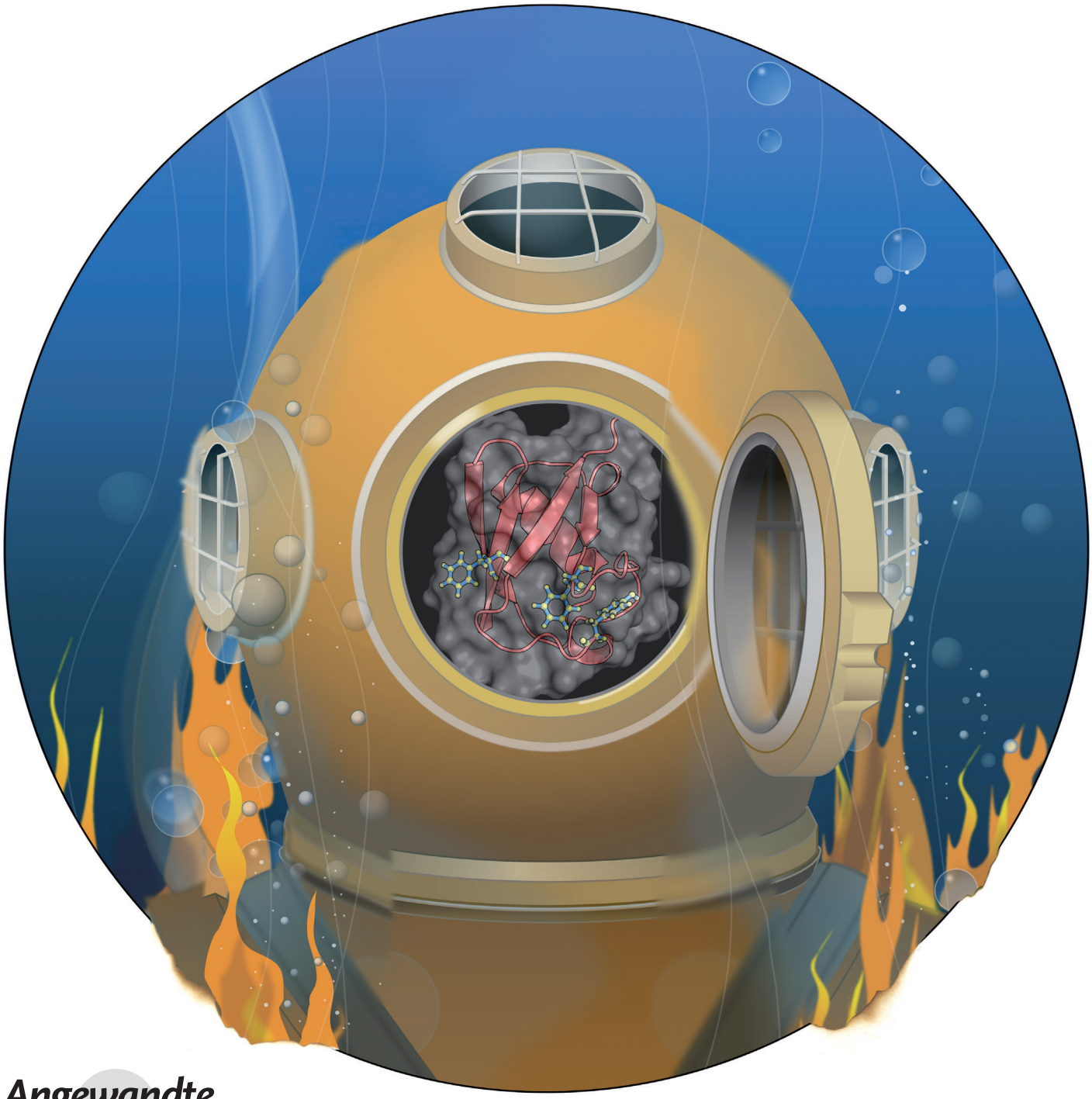

Abstract: *Aromatic amino acid side chains have a rich role within proteins and are often central to their structure and function. Suitable isotopic-labelling strategies enable studies of sub-nanosecond aromatic-ring dynamics using solution NMR relaxation methods. Surprisingly, it was found that the three aromatic side chains in human ubiquitin show a sharp thermal dynamical transition at approximately 312 K. Hydrostatic pressure has little effect on the low-temperature behavior, but somewhat decreases the amplitude of motion in the high-temperature regime. Therefore, below the transition temperature, ring motion is largely librational. Above this temperature, a complete ring-rotation process that is fully consistent with a continuous diffusion not requiring the transient creation of a large activated free volume occurs. Molecular dynamics simulations qualitatively corroborate this view and reinforce the notion that the dynamical character of the protein interior has much more liquid-alkane-like properties than previously appreciated.*

Aromatic amino acid side chains have a rich structural role within proteins[1] and are often central to their biological function, particularly in the context of molecular recognition[2] and catalysis.[3] Thus the motional character of aromatic residues would seem to be of central importance in a range of protein structure–function issues. In this context, solution NMR spectroscopy has a long history in the investigation of aromatic-ring dynamics in proteins. Early investigations were largely restricted to information about motion on the millisecond to second time scale as manifested in line broadening or population exchange phenomena.[4] Symmetry considerations suggested that slowly moving Phe and Tyr rings were "flipping" about the associated $\chi 2$ torsion angle. The temperature[5] and pressure[6] dependence of the rate of ring flipping further suggested a jump-like rather than continuous diffusive motion with a high enthalpy barrier and a large activated volume. As pointed out recently,[7] experimental measurements of ring-flip rates have been limited to the handful of cases where separate peaks are observed for symmetry-related nuclei and constitute a very small fraction of the aromatic resonances that have been reported. In the past, aromatic rings that do not show line broadening or non-degenerate symmetry related resonances were generally assumed to be flipping at rates much faster than the anticipated difference in the chemical shifts of the interchanged nuclei, that is, at greater than $10^3\ s^{-1}$. Absent from this classical view is insight into more restricted (i.e., librational) motion within a rotamer well.

Recently, there has been a renaissance of interest in the details of aromatic-ring motion with the introduction of new experimental strategies that have broadened the spectrum of insight available. Particularly noteworthy is the use of supercooled water to access temperatures where aromatic-ring dynamics with low activation enthalpies can be more favorably studied using line broadening and chemical exchange phenomena.[5] More recently, a number of isotopic-labeling strategies have been introduced to enable relaxation studies to probe the picosecond/nanosecond and microsecond/millisecond time scales.[8] These labeling schemes are designed to ameliorate confounding spin–spin interactions that have previously limited measurements of ^{13}C relaxation in aromatic-ring systems to natural abundance.[9]

Herein, we use ^{13}C relaxation to characterize the fast internal motion of Phe and Tyr ring systems in the protein ubiquitin as a function of hydrostatic pressure and temperature. Ubiquitin is a small protein (76 residues) essential to the eukaryotic ATP-dependent protein degradation pathway.[11] For such a small protein, ubiquitin displays a surprising range of secondary structures, including a five-stranded mixed β-sheet, α- and 3_{10}-helices, and a number of tight turns.[10] The protein also contains three aromatic residues: Phe-4, Phe-45, and Tyr-59. These residues are largely buried (Figure 1).

For classical relaxation phenomena used to probe sub-nanosecond motions, aromatic residues present a difficult situation. Aside from the concern about the isolation of the spin interaction of interest from extraneous contributions, aromatic ring systems suffer from extensive homo- and heteronuclear scalar interactions, which can also complicate relaxation data. To isolate a ^1H–^{13}C pair in the aromatic ring in an otherwise perdeuterated background we used a biosynthetic scheme based on [$^{13}C_4$]-eyrthrose.[8b] The protein was also uniformly labeled with ^{15}N.[12]

Measurements of ^{13}C relaxation were carried out using standard pulse sequences. Relaxation data was obtained at 283, 293, 303, 308, 313, 323, and 328 K at ambient pressure. Relaxation measurements were also made at elevated pressures of 1200 and 2500 bar at 283, 303, and 323 K using

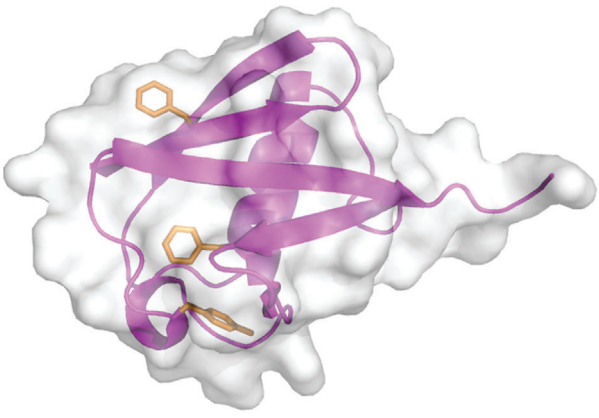

Figure 1. Ribbon representation of ubiquitin (PDB code: 1UBQ)[10] with surface rendering. The side chains of Phe-4, Phe-45, and Tyr-59 are shown from top to bottom as orange stick models. These residues have solvent-accessible surface areas of 55 Å^2 (31%), 36 Å^2 (21%), and 39 Å^2 (21%). Structure drawn with PyMol.

[*] V. Kasinath, Dr. Y. Fu, Prof. K. A. Sharp, Prof. A. J. Wand
Department of Biochemistry & Biophysics
University of Pennsylvania
Philadelphia, PA 19104 (USA)
E-mail: wand@upenn.edu

[**] This work was supported by the NIH (GM102447) and, in part, by a grant from the G. Harold & Leila Y. Mathers Foundation. A.J.W. declares a competing financial interest as a Member of Daedalus Innovations, LLC, a manufacturer of high-pressure NMR apparatus.

Supporting information for this article is available on the WWW under http://dx.doi.org/10.1002/anie.201408220.

procedures described elsewhere.[12] The ^{15}N and ^{13}C relaxation data was analyzed using the model-free treatment of Lipari and Szabo,[13] as described previously.[8b] ^{15}N relaxation data was obtained to determine macromolecular tumbling and analyzed as described in detail elsewhere[12] (Supporting Information, Tables S1 and S2). Based on ^{15}N relaxation, the determined tumbling models were fully anisotropic at 283 and 303 K at all pressures (1, 1200, and 2500 bar) whereas those at 313 and 323 K were axially symmetric at all pressures (Table S1). The fitted Lipari–Szabo squared generalized order parameters (O^2) and associated effective correlation times (τ_e) for the ^1H–$^{13}C_5$ aromatic bond vectors were of high precision (Figure 2 and Figure 3; see also Tables S3 and S4).

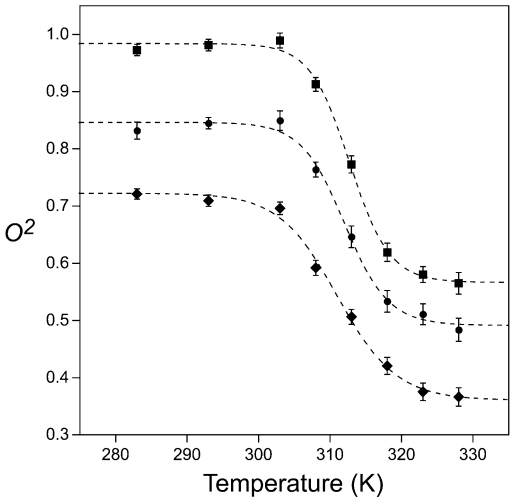

Figure 2. Experimentally observed temperature dependence of aromatic-ring motion in ubiquitin on the picosecond/nanosecond time scale. Lipari–Szabo O^2 parameters of the C_5–H ring bond vectors of Tyr-59 (■), Phe-4 (◆), and Phe-45 (●) determined by ^{13}C relaxation. The dashed lines are fitted sigmoidal curves.

Classical NMR relaxation of the type used here probes motions on a time scale faster than macromolecular tumbling, which is on the order of 3 ns. At low temperatures, the O^2 parameters of the C_5–H bond vectors of Phe-4, Phe-45 and Tyr-59 are high, with that of Tyr-59 being close to the theoretical limit of 1 indicating nearly complete rigidity within the molecular frame. There is little temperature dependence of the order parameters up to approximately 303 K where a sharp transition to lower values begins. All three aromatic rings display this transition, which is complete by 330 K. The fitted midpoint of this transition is approximately 312 ± 1 K, which is well below the thermal unfolding transition observed by calorimetry.[14] The sharpness of the observed dynamical transition suggests that the associated activation enthalpy is small. Indeed, there is only the barest hint of it in the pre-transition region of the differential scanning calorimetry trace of the protein.[14] It should again be noted that the protein undergoes a slight change in hydrodynamic character in this temperature range (Table S1), but this does not influence the interpretation of the observed relaxation data (Table S5).

Following the dynamical transition centered around 310 K, the order parameters of the probes for all three aromatic rings settle at significantly lower values (Figure 2). The order parameters appear to be temperature-independent above the transition. It is tempting to treat the dynamical transition as a two-state phenomenon and undertake a van't Hoff analysis. This leads to an obviously erroneous activation enthalpy of approximately 30 kcal mol^{-1} (not shown). The temperature dependence of the effective correlation times associated with this dynamical transition indicates why a simple two-state view is inappropriate. During the transition, the fitted τ_e values increase substantially (Figure 3; see below). The effective correlation time of Tyr-59 undergoes an extremely sharp transition with an apparent midpoint of 305 ± 2 K. Phe-4 and Phe-45 both show a more gradual transition in effective correlation times with similar midpoint temperatures (ca. 314 ± 2 K).

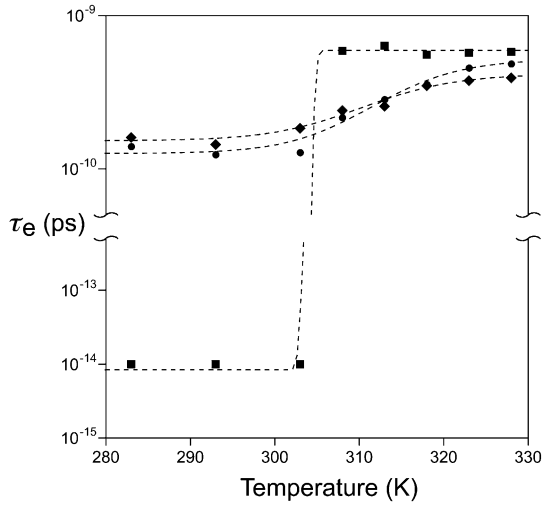

Figure 3. Experimentally observed temperature dependence of aromatic-ring motion in ubiquitin on the picosecond/nanosecond time scale. Semi-logarithmic plot of the Lipari–Szabo effective correlation times of the motion of the C_5–H ring bond vectors of Tyr-59 (■), Phe-4 (◆), and Phe-45 (●) determined by ^{13}C relaxation. The fitted errors are smaller than the size of the symbols. The dashed lines are fitted sigmoidal curves.

The sharpness of the thermally induced transition of fast motion of the aromatic rings would suggest the onset of a qualitatively different motion. The rigid nature of the aromatic ring allows for relatively straightforward modeling of the influence of available motions about the connected $\chi 1$ and $\chi 2$ torsion angles on the obtained O^2 parameter.[15] Steric considerations suggest that motion about $\chi 1$ can be neglected. At temperatures below the dynamical transition, the high values of O^2 strongly suggest the absence of aromatic-ring rotation or flipping and that the ring is undergoing librational motion. The restricted diffusion model of Wittebort and Szabo[16] predicts libration angles of 9°, 27°, and 39° for Tyr-59, Phe-45, and Phe-4, respectively. These are remarkably large excursions. There is very little temperature dependence indicating an essentially free diffusive motion. The dynamical

transition most likely results from the onset of rotation of the aromatic ring as this is the only reasonable physical mechanism for reducing the O^2 parameter to values of 0.5 and below.[15] It is important to note that the motions of methyl-bearing side chains generally show a small, linear dependence in this temperature range.[17]

To substantiate this interpretation, molecular dynamics simulations of ubiquitin were carried out at 283, 293, 303, 308, 313, and 323 K. The simulations qualitatively reproduced the effect of temperature on the O^2 values, but with some differences (Figure S1). Below 300 K, the order parameters of the three aromatic groups are high. With increasing temperature, O^2 for both Phe residues decreases sharply and in concert to a low value above 300 K. However, O^2 for Tyr-59 does not decrease over the temperature range 283–323 K, in contrast to experimental results. The tyrosine hydroxy group participates both as a hydrogen bond acceptor and donor. The poor correspondence between experiment and simulation may arise from this feature. Simulations carried out at 353 K also failed to show the Tyr-59 ring flipping. In contrast, the temperature dependence of O^2 for the two Phe residues is almost identical, in agreement with experiment, although the transition from high to low O^2 values occurs at approximately 10 K lower values. The dynamic behavior of the two Phe residues was then examined in detail. For temperatures of less than 300 K, O^2 values were determined almost entirely by approximately 15° librations around the $\chi 2$ angle. No ring flips were seen in 120 ns of simulation. The libration has a very fast time scale, with $\tau_t < 1$ ps (Figure S2). As T increases above 300 K, both Phe residues undergo ring flips with increasing frequency. Ring flipping is several orders of magnitude slower than libration (Figure S2) and only contributes significantly to relaxation at higher temperature (Figure S7). This explains why the data in Figures 2 and 3 show lower values of O^2, but a larger overall τ_e value at higher temperature. To determine whether the parallel temperature dependence of the two Phe residues indicated cooperative behavior, the correlation between ring flips was examined. For each flip in either Phe-4 or Phe-45, the time delay (positive or negative) between it and the closest flip of the other residue was determined. From this, the mean delay time $< \delta t >$ over the 120 ns simulation was computed. $< \delta t >$ was statistically indistinguishable from that expected from two completely independent, stochastic events. No evidence of direct Phe–Phe correlation in ring-flip dynamics was detectable. We next addressed the mechanism of temperature activation of ring flipping. In a solid-state view of a well-packed native protein, an increase in temperature promotes increased amplitude and frequency of packing defects, which could then permit more frequent ring flipping. An examination of both the overall packing efficiency and the packing efficiency of the Phe-4 and Phe-45 side chains showed no support for this model for ring-flip activation: Temperature had no significant effect on the average packing or fluctuations in packing (Figure S3). A more nuanced and physically realistic measure of packing comes from the van der Waals (vdw) contribution to the pressure virial,[18] $v_{ij} = r_{ij} U_{ij}$, where r_{ij} and U_{ij} are the distance and interaction potential, respectively, between atoms i and j. The repulsive and attractive parts of the vdw term of the pressure virial are shown in Figure S4. There is no significant change over the temperature range of 293 K to 303 K where the ring flipping becomes active. Together, the simulations support the view of aromatic rings undergoing independent, stochastic ring flipping in a "liquid-like" environment.

The application of hydrostatic pressure has been used in the past to investigate the volumetric properties of slow ring-flipping processes in proteins.[6] In the few cases examined, the associated activation volumes are large and range from approximately 30 to 50 mL mol^{-1}. In distinct contrast, the application of hydrostatic pressure hardly affects the fast ring motion observed in ubiquitin (Figure 4). Below the thermal

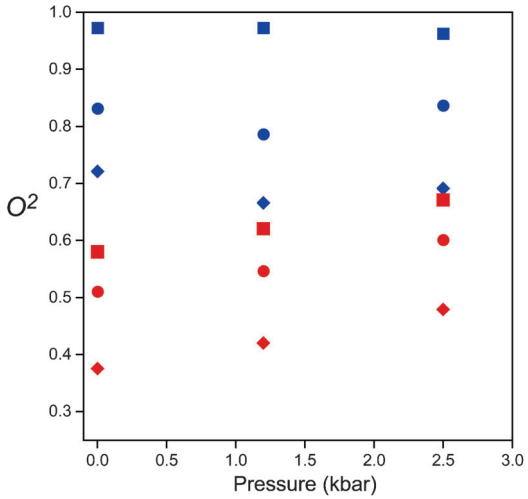

Figure 4. Experimentally observed pressure sensitivity of aromatic-ring motion in ubiquitin above and below the thermal transition temperature for ring flipping. Lipari–Szabo O^2 parameters of the C_5–H ring bond vectors of Tyr-59 (■), Phe-4 (◆), and Phe-45 (●) determined by ^{13}C relaxation at 283 K (blue) and 323 K (red).

transition temperature, the O^2 parameters decrease slightly, which corresponds to a reduction in the effective restricted diffusion angles by 3° or less at the highest pressure examined. The corresponding effective correlation times are similarly insensitive to the applied pressure. Above the thermal transition temperature, where fast ring flipping or rotation is present, the pressure sensitivities of the O^2 parameters of all three rings are significant. It is important to remember that the order parameter is a measure of equilibrium fluctuations.[13] Thus, its sensitivity to pressure indicates the presence of a significant contribution of large-amplitude continuous diffusion to the high-temperature motion as a pure jump-like ring-flip motion interconverts two identical (for Phe) and nearly identical (for Tyr) states and would be predicted to be insensitive to pressure. Interestingly, the motions of the methyl-bearing side chains closest to the aromatic rings show a non-linear experimental pressure dependence.[12]

The associated effective correlation times for ring motion above the dynamical transition temperature are also quite responsive to hydrostatic pressure. Unfortunately, the interpretation of the effective correlation time is fraught with qualifications.[13] The effective correlation time depends both on the microscopic diffusion or jump constants and the spatial

nature of the motion. Furthermore, for the diffusive motion evident here, the internal correlation function is potentially defined as an infinite sum of exponentials[13,19] and cannot be associated with a simple rate constant. Nevertheless, the increase in effective correlation times is consistent with the thermally induced motions being somewhat slower than the more restricted motion seen below the transition temperature.

MD simulations reproduce the qualitative effects of pressure on the Phe order parameters well (Figure S5). Below the transition temperature, the order parameters are high, and pressure has no significant effect. Above the transition temperature, the order parameters increase sharply as the pressure is increased to 2500 bar. This increase is not accompanied by any significant change in either the packing of the protein, globally or around the Phe residues, nor by any change in the volume fluctuations. A consideration of the pressure sensitivity of the order parameters indicates that the thermally induced dynamical transition involves the onset of a qualitatively distinct larger amplitude but still diffusive rotation of the aromatic rings. This view is in contrast to that seen in slowly interconverting systems where ring rotation is characterized by discrete jumps, high activation volumes, and large activation enthalpies.[6] The large-scale diffusive motions identified here clearly indicate that the protein interior is more liquid-like than perhaps previously appreciated. From a liquid-state perspective, the viscous properties of the protein interior would be more important than packing or volume fluctuations. It is well known that pressures in the range of 1200–2500 bar can increase the viscosity of liquid alkanes by a factor of 4–5 with only 14–16% changes in density.[20] Similar magnitude changes operating in the apolar core of ubiquitin would account for the effects seen here. Finally, it is striking that the thermal activation processes of all three aromatic ring systems in ubiquitin share a common transition temperature, which corresponds to the physiological temperature. The generality of this observation remains to be determined.

Experimental Section

NMR sample preparation: Human ubiquitin was expressed during growth on M9 minimal media prepared in 99% D_2O with 1.0 $g\,L^{-1}$ of $^{15}NH_4Cl$ and 2.0 $g\,L^{-1}$ of ^{12}C/deuterated pyruvate and supplemented at an OD_{600} of 0.5 with 1.0 $g\,L^{-1}$ of [$^{13}C_4$]-erythrose as described previously.[8b] The protein was purified as described previously[21] and yielded 9 $mg\,L^{-1}$. Labeling was confirmed by NMR analysis (Figure S6). Uniformly ^{15}N-enriched ubiquitin with [$^{13}C_5$]-labeled aromatic residues (1.0 mM) was prepared in a solution at pH 5.0 containing NaOAc (50 mM), NaCl (50 mM), NaN_3 (0.02% w/v), and D_2O (8%).

NMR relaxation experiments: Uniformly ^{15}N-enriched ubiquitin with [$^{13}C_5$]-labeled aromatic residues (1.0 mM) was prepared in a solution at pH 5.0 containing NaOAc (50 mM), NaCl (50 mM), NaN_3 (0.02% w/v), and D_2O (8%). Relaxation experiments were carried out on Bruker Avance III NMR spectrometers equipped with cryoprobes and operating at 500 and 600 MHz (^1H) essentially as described previously.[8b] High-pressure NMR experiments were carried out using a 2.5 kbar rated NMR cell (3.0 mm inner diameter/5.0 mm outer diameter) and an Xtreme-60 automated pressure generator (Daedalus Innovations, Aston, PA). Further details regarding data acquisition are provided in the Supporting Information.

Relaxation data analysis: Backbone motion and macromolecular tumbling analysis[22] was based on ^{15}N relaxation obtained at 10, 30, 40, and 50°C as described elsewhere using trimmed data sets and pairwise comparisons of obtained F values.[12] Tumbling of ubiquitin was fully anisotropic at 10 and 30°C and at all pressures examined (1, 1200, and 2500 bar) whereas at 40 and 50°C and all pressures examined, tumbling was axially symmetric (see Table S1). As the viscosity of water varies smoothly between 10 and 60°C, tumbling times at intermediate temperatures were obtained by interpolation (see Table S2). Lipari–Szabo model-free squared generalized order parameters (O^2) and effective correlation times (τ_e) were determined using a grid-search[23] approach using in-house software.[8b] An effective C–H bond length of 1.09 Å and residue-specific chemical shift anisotropy tensors with axially symmetric and anisotropic CSA values for Phe and Tyr, respectively, were employed.[24] An effective N–H bond length of 1.04 Å and a ^{15}N chemical shift anisotropy tensor breadth of −170 ppm were used. The precision of model-free parameters was estimated using Monte Carlo sampling based on the experimental precision of relaxation observables.

Molecular dynamics simulations: Simulations were performed using the NAMD simulation package, the CHARMM27 potential function, a solvent boundary of at least 5 Å of explicit TIP3P water, particle mesh Ewald boundary conditions, at constant temperature and a pressure of 1 bar for a time of 120 ns at each temperature. Other simulation details and the calculations of the O^2 and τ_c values are described elsewhere.[25]

Received: August 14, 2014
Published online: December 4, 2014

Keywords: conformational analysis · NMR spectroscopy · protein dynamics · relaxation · thermal activation

[1] a) K. A. Thomas, G. M. Smith, T. B. Thomas, R. J. Feldmann, *Proc. Natl. Acad. Sci. USA* **1982**, *79*, 4843–4847; b) S. K. Burley, G. A. Petsko, *Science* **1985**, *229*, 23–28; c) S. K. Burley, G. A. Petsko, *FEBS Lett.* **1986**, *203*, 139–143; d) K. A. Dill, *Biochemistry* **1990**, *29*, 7133–7155.
[2] a) S. Birtalan, R. D. Fisher, S. S. Sidhu, *Mol. BioSyst.* **2010**, *6*, 1186–1194; b) A. A. Bogan, K. S. Thorn, *J. Mol. Biol.* **1998**, *280*, 1–9.
[3] G. J. Bartlett, C. T. Porter, N. Borkakoti, J. M. Thornton, *J. Mol. Biol.* **2002**, *324*, 105–121.
[4] K. Wüthrich, G. Wagner, *FEBS Lett.* **1975**, *50*, 265–268.
[5] J. J. Skalicky, J. L. Mills, S. Sharma, T. Szyperski, *J. Am. Chem. Soc.* **2001**, *123*, 388–397.
[6] a) G. Wagner, *FEBS Lett.* **1980**, *112*, 280–284; b) M. Hattori, H. Li, H. Yamada, K. Akasaka, W. Hengstenberg, W. Gronwald, H. R. Kalbitzer, *Protein Sci.* **2004**, *13*, 3104–3114.
[7] U. Weininger, M. Respondek, C. Low, M. Akke, *J. Phys. Chem. B* **2013**, *117*, 9241–9247.
[8] a) K. Teilum, U. Brath, P. Lundstrom, M. Akke, *J. Am. Chem. Soc.* **2006**, *128*, 2506–2507; b) V. Kasinath, K. G. Valentine, A. J. Wand, *J. Am. Chem. Soc.* **2013**, *135*, 9560–9563; c) R. J. Lichtenecker, K. Weinhaupl, W. Schmid, R. Konrat, *J. Biomol. NMR* **2013**, *57*, 327–331.
[9] A. G. Palmer, R. A. Hochstrasser, D. P. Millar, M. Rance, P. E. Wright, *J. Am. Chem. Soc.* **1993**, *115*, 6333–6345.
[10] S. Vijay-Kumar, C. E. Bugg, W. J. Cook, *J. Mol. Biol.* **1987**, *194*, 531–544.
[11] M. H. Glickman, A. Ciechanover, *Physiol. Rev.* **2002**, *82*, 373–428.
[12] Y. Fu, V. Kasinath, V. R. Moorman, N. V. Nucci, V. J. Hilser, A. J. Wand, *J. Am. Chem. Soc.* **2012**, *134*, 8543–8550.

[13] G. Lipari, A. Szabo, *J. Am. Chem. Soc.* **1982**, *104*, 4546 – 4559.
[14] B. Ibarra-Molero, V. V. Loladze, G. I. Makhatadze, J. M. Sanchez-Ruiz, *Biochemistry* **1999**, *38*, 8138 – 8149.
[15] R. M. Levy, R. P. Sheridan, *Biophys. J.* **1983**, *41*, 217 – 221.
[16] R. J. Wittebort, T. M. Rothgeb, A. Szabo, F. R. Gurd, *Proc. Natl. Acad. Sci. USA* **1979**, *76*, 1059 – 1063.
[17] X. J. Song, P. F. Flynn, K. A. Sharp, A. J. Wand, *Biophys. J.* **2007**, *92*, L43 – 45.
[18] M. P. Allen, D. J. Tildesley, *Computer Simulations of Liquids*, Clarendon, Oxford, **1990**.
[19] R. J. Wittebort, A. Szabo, *J. Phys. Chem.* **1978**, *69*, 1722 – 1736.
[20] D. W. Brazier, G. R. Freeman, *Can. J. Chem.* **1969**, *47*, 893 – 899.
[21] A. J. Wand, J. L. Urbauer, R. P. McEvoy, R. J. Bieber, *Biochemistry* **1996**, *35*, 6116 – 6125.
[22] N. Tjandra, S. E. Feller, R. W. Pastor, A. Bax, *J. Am. Chem. Soc.* **1995**, *117*, 12562 – 12566.
[23] M. J. Dellwo, A. J. Wand, *J. Am. Chem. Soc.* **1989**, *111*, 4571 – 4578.
[24] C. H. Ye, R. Q. Fu, J. Z. Hu, L. Hou, S. W. Ding, *Magn. Reson. Chem.* **1993**, *31*, 699 – 704.
[25] a) V. Kasinath, K. A. Sharp, A. J. Wand, *J. Am. Chem. Soc.* **2013**, *135*, 15092 – 15100; b) N. V. Prabhu, A. L. Lee, A. J. Wand, K. A. Sharp, *Biochemistry* **2003**, *42*, 562 – 570.

